HHS Public Access

Author manuscript

Gastroenterology. Author manuscript; available in PMC 2024 September 01.

Published in final edited form as:

Gastroenterology. 2023 September ; 165(3): 656–669.e8. doi:10.1053/j.gastro.2023.05.041.

Hypusination Maintains Intestinal Homeostasis and Prevents Colitis and Carcinogenesis by Enhancing Aldehyde Detoxification

Alain P. Gobert[1,2,3], **Thaddeus M. Smith**[1], **Yvonne L. Latour**[1,4], **Mohammad Asim**[1], **Daniel P. Barry**[1], **Margaret M. Allaman**[1], **Kamery J. Williams**[1], **Kara M. McNamara**[1,3], **Alberto G. Delgado**[1], **Sarah P. Short**[1,2], **Raghavendra G. Mirmira**[5], **Kristie L. Rose**[6], **Kevin L. Schey**[6], **Irene Zagol-Ikapitte**[7,8], **Jeremy S. Coleman**[7,8], **Olivier Boutaud**[7,8], **Shilin Zhao**[9], **M. Blanca Piazuelo**[1,2], **M. Kay Washington**[2,4], **Lori A. Coburn**[1,2,3,10], **Keith T. Wilson**[1,2,3,4,10]

[1]Division of Gastroenterology, Hepatology, and Nutrition, Department of Medicine, Vanderbilt University Medical Center, Nashville, TN, USA.

[2]Center for Mucosal Inflammation and Cancer, Vanderbilt University Medical Center, Nashville, TN, USA.

[3]Program in Cancer Biology, Vanderbilt University Medical Center, Nashville, TN, USA.

[4]Department of Pathology, Microbiology, and Immunology, Vanderbilt University Medical Center, Nashville, TN, USA.

[5]Kovler Diabetes Center, Department of Medicine, The University of Chicago, Chicago, IL, USA.

[6]Department of Biochemistry, Mass Spectrometry Research Center, Vanderbilt University School of Medicine, Nashville, TN, USA.

[7]Warren Center for Neuroscience Drug Discovery, Vanderbilt University, Nashville, TN, USA.

[8]Department of Pharmacology, Vanderbilt University School of Medicine, Nashville, TN, USA.

[9]Department of Biostatistics, Vanderbilt University Medical Center, Nashville, TN 37232, USA.

[10]Veterans Affairs Tennessee Valley Healthcare System, Nashville, TN, USA

Abstract

Correspondence: Alain P. Gobert, Vanderbilt University Medical Center, 2215B Garland Ave., 1015C MRB IV, Nashville, TN 37232-0252. Phone 615-343-5577; alain.p.gobert@vumc.org; Keith T. Wilson, Vanderbilt University Medical Center, 2215B Garland Ave., 1030C MRB IV, Nashville, TN 37232-0252. Phone 615-343-5675; keith.wilson@vumc.org.

Author Contributions: Conceptualization, A.P.G., and K.T.W.; Formal Analysis, A.P.G., Y.L.L., K.L.R., K.L.S., O.B., S.Z.; Investigation, A.P.G, T.M.S., Y.L.L., M.A., D.P.B., M.M.A., K.J.W., K.M.M., A.G.D., S.P.S., I.Z-I, M.B.P., M.K.W., and L.A.C.; Resources, J.S.C., R.G.M.; Visualization, A.P.G.; Writing - Original Draft, A.P.G.; Writing - Review & Editing, A.P.G., L.A.C., and K.T.W.; Visualization, A.P.G.; Supervision, A.P.G. and K.T.W.; Funding Acquisition, A.P.G. and K.T.W.

Disclosures: APG and KTW are named inventors on a patent application for the use of electrophile scavengers. In addition, APG and KTW are named on a licensing agreement between Vanderbilt University and MTI Biotech, Inc. for the future use of electrophile scavengers. All other authors have declared that no conflict of interest exists.

BACKGROUND & AIMS: The amino acid hypusine, synthesized from the polyamine spermidine by the enzyme deoxyhypusine synthase (DHPS), is essential for the activity of eukaryotic translation initiation factor 5A (EIF5A). The role of hypusinated EIF5A (EIF5A^{Hyp}) remains unknown in intestinal homeostasis. Our aim was to investigate EIF5A^{Hyp} in the gut epithelium in inflammation and carcinogenesis.

METHODS: We utilized human colon tissue mRNA samples and publicly-available transcriptomic datasets, tissue microarrays, and patient-derived colon organoids. Mice with intestinal epithelial-specific deletion of *Dhps* were investigated at baseline and in models of colitis and colon carcinogenesis.

RESULTS: We found that patients with ulcerative colitis and Crohn's disease exhibit reduced colon levels of *DHPS* mRNA and DHPS protein, and reduced levels of EIF5A^{Hyp}. Similarly, colonic organoids from colitis patients also show downregulated *DHPS* expression. Mice with intestinal epithelial-specific deletion of *Dhps* develop spontaneous colon hyperplasia, epithelial proliferation, crypt distortion, and inflammation. Furthermore, these mice are highly susceptible to experimental colitis and show exacerbated colon tumorigenesis when treated with a carcinogen. Transcriptomic and proteomic analysis on colonic epithelial cells demonstrated that loss of hypusination induces multiple pathways related to cancer and immune response. Moreover, we found that hypusination enhances translation of numerous enzymes involved in aldehyde detoxification, including glutathione S-transferases and aldehyde dehydrogenases. Accordingly, hypusination-deficient mice exhibit increased levels of aldehyde adducts in the colon, and their treatment with a scavenger of electrophiles reduces colitis.

CONCLUSIONS: Hypusination in intestinal epithelial cells has a key role in prevention of colitis and colorectal cancer, and enhancement of this pathway via supplementation of spermidine could have therapeutic impact.

Graphical Abstract

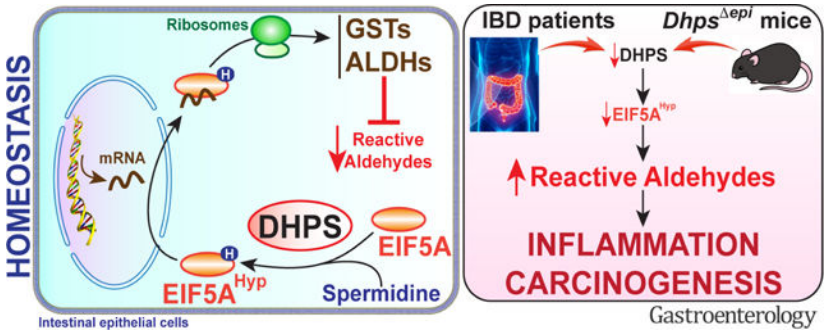

Keywords

Hypusine; Intestinal epithelial cells; Inflammation; Colon cancer

Introduction

The prevalence of inflammatory bowel disease (IBD), including Crohn's disease (CD) and ulcerative colitis (UC), is increasing considerably worldwide, especially in countries with

the largest populations, such as USA, India, and China.[1,2] Newer biologic therapies for IBD have been developed and extensively used, but they induce remission in only about half of patients, are expensive, and have various side effects. Moreover, colonic inflammation is also a risk factor for colitis-associated carcinoma (CAC) that accounts for approximately 15% of all deaths in IBD patients.[3] Thus, a better understanding of the molecular events contributing to inflammation and neoplastic transformation would benefit IBD patients.

Polyamines are organic cations and the first one, putrescine, is generated by the enzymatic decarboxylation of arginine and ornithine by the arginine decarboxylase/agmatinase pathway and the enzyme ornithine decarboxylase, respectively. Putrescine is converted into spermidine (Spd), which is then transformed into spermine. The enzyme spermine oxidase (SMOX) catalyzes the back-conversion of spermine to Spd.[4] We have shown that patients with colitis have reduced SMOX expression and that mice with *Smox* deletion exhibit decreased colonic Spd and an exacerbation of colitis[5,6] and CAC.[6] Treatment of animals with Spd ameliorates both diseases and protects mice with epithelial deletion of *Apc* from tumorigenesis.[6] The enzyme deoxyhypusine synthase (DHPS) transfers the N-terminal moiety of Spd to the lysine-50 residue of the protein eukaryotic translation initiation factor 5A (EIF5A) to form the intermediate deoxyhypusine residue;[7] then deoxyhypusine hydroxylase (DOHH) catalyzes the hydroxylation of this intermediate[8] to complete the synthesis of the nonproteinogenic amino acid hypusine. Thus, EIF5A is the only known protein that contains hypusine. Hypusinated EIF5A ($EIF5A^{Hyp}$) enters the nucleus via passive diffusion and binds specific mRNAs exhibiting a 5′-AAAUGU-3′ consensus sequence.[9,10] $EIF5A^{Hyp}$/mRNA complexes are then translocated to the cytoplasm by the nuclear transporter exportin-4[11] and reach the ribosomes for translation.[12] $EIF5A^{Hyp}$ also alleviates ribosome pausing during the translation of peptides enriched in diprolyl and diglycyl motifs.[13,14] Hypusination is crucial for embryogenesis and deletion of *Eif5a1* or *Dhps* is lethal.[15] Because hypusination supports cell differentiation and proliferation,[16,17] it has been proposed that this pathway could represent a potential target to limit tumor progression.[18] Chemical inhibition of DHPS using the competitive Spd analog N1-guanyl-1,7-diamineheptane (GC7) or knockdown of the genes encoding for EIF5A or DHPS reduces the growth of established cancer cell lines in vitro and in xenograft models.[18,19] However, the effect of hypusination on inflammation and carcinogenesis in non-transformed epithelial cells, notably in the gastrointestinal tract, remains unknown.

We found that mice with specific deletion of *Dhps* in intestinal epithelial cells (IECs) exhibit spontaneous intestinal inflammation, are highly susceptible to dextran sulfate sodium (DSS)-induced colitis and to the azoxymethane (AOM)-DSS protocol and develop more tumors in a model of colorectal cancer driven by AOM alone. We demonstrate that epithelial $EIF5A^{Hyp}$ regulates the translation of enzymes involved in reactive aldehyde detoxification, leading to the development of a proinflammatory and procarcinogenic profile in colonic epithelial cells (CECs) lacking DHPS. Human translational relevance is supported by our findings that the levels of *DHPS* mRNA are decreased in IBD patient colon tissues, levels of DHPS and $EIF5A^{Hyp}$ in CECs are reduced in these tissues, and colon organoids from patients with colitis exhibit decreased *DHPS* expression compared to controls. Moreover, administration of a scavenger of reactive aldehydes ameliorated DSS-induced colitis in *Dhps* epithelial-specific knockout mice. Thus, enhancement of the hypusination pathway by

supplementation with the DHPS substrate, Spd, and/or detoxification of reactive aldehydes are potential treatments for IBD and chemopreventive methods for prevention of CAC and CRC.

Methods

Ethics Statement

The ethics statements regarding human tissues and animal experiments are provided in the Supplementary Methods.

Database Analysis

Series matrix files were analyzed by GEO2R from the GEO database (http://www.ncbi.nlm.nih.gov/geo/).

Mice and Models of Colitis and Colon Cancer

Animals were house bred in our animal facility and were fed with 5L0D chow (LabDiet). To achieve specific deletion of *Dhps* in IECs, we crossed C57BL/6J $Dhps^{fl/fl}$ mice, in which exons 2 to 7 of the *Dhps* gene were flanked by Cre recombinase recognition sequences,[20] to transgenic mice overexpressing the epithelial driver $Vil1^{cre}$ (Strain 021504; The Jackson Laboratory). The resulting $Dhps^{+/fl}$;$Vil1^{cre}$ mice were then crossed to $Dhps^{fl/fl}$ mice to create $Dhps^{fl/fl}$;$Vil1^{cre}$ mice (46% of offspring), termed $Dhps^{\Delta epi}$, and the littermate $Dhps^{fl/fl}$ mice (54% of offspring), which were used as controls. Littermate co-housed $Dhps^{fl/fl}$ and $Dhps^{\Delta epi}$ female and male mice (8–12 wk) were used for all the experiments.

For the colitis model, age-matched (8–12 wk) female and male mice were treated with 2%–4% DSS (mol. wt. 36,000–50,000; TdB Labs) in the drinking water for 5 days; DSS was then removed, and mice were maintained on regular water until euthanasia. For the CAC model, animals received one intraperitoneal (i.p.) injection of 12.5 mg/kg AOM (Millipore) followed by 3 cycles of 1.7%–3% DSS for 4 days beginning at day 5, 26, and 47[6,21] and mice were euthanized on day 56 or sooner if moribund. In an additional model, mice were treated every wk with an i.p. injection of 12.5 mg/kg AOM for 3 or 6 consecutive wks and were euthanized 127 days after the first injection.[22] Animals were also treated with 1.5 mg/ml 5-ethyl-2-hydroxybenzylamine (EtHOBA), a potent scavenger of dicarbonyl electrophiles,[21,23,24] in the drinking water one wk before DSS and were also maintained on EtHOBA during DSS treatment and the recovery period.[29]

Mice were monitored daily and weighed daily for the DSS model and weekly for the CAC model. Animals showing extreme distress, that became moribund, or lost more than 20% of initial body weight were euthanized. After sacrifice, colons were removed, measured, dissected, and Swiss-rolled for histology. In the cancer models, tumors were also counted and measured in two dimensions in the distal colon with electronic calipers under a dissecting microscope.[6,21,25] Tumor burden was determined by the sum of areas of all tumors.

Histology

Swiss-rolled colons were fixed in formalin and embedded in paraffin, and 5 μm sections were stained with hematoxylin and eosin (H&E) and examined in a blinded manner by a gastrointestinal pathologist (M.K.W.). Histological injury score (0–40) and severity of dysplasia in the AOM model were determined as described.[6,21,25]

Immunostaining

The details regarding immunohistochemistry (IHC) and immunofluorescence (IF) are provided in the Supplementary Methods.

Isolation of CECs

The details are provided in the Supplementary Methods.

Colon Organoids

The methods used to generate and stimulate colon organoids are provided in the Supplementary Methods.

Analysis of mRNA Expression

RNA sequencing (RNA-Seq) and RT-PCR are described in the Supplementary Methods.

Protein Expression Analysis

Proteomic analysis and Western blotting are described in the Supplementary Methods.

Measurement of Glutathione-S-transferase (GST) Activity

Colonoids were treated or not with 25 μM GC7 for 24 h. Proteins were then extracted and quantified as reported.[26] The activity of the total GST activity in protein lysates (10 μg) was measured using the GST Assay Kit (LSBio).

Quantification of Dicarbonyl Electrophile Adducts

The measurement of the crosslinks of malondialdehyde (MDA) to lysine (dilysyl-MDA) was performed by mass spectrometry, as described in the Supplementary Methods.

Fecal Microbiota Analysis

Littermate co-housed $Dhps^{fl/fl}$ and $Dhps^{\Delta epi}$ mice (9 wks) were sacrificed, and feces present in the colon were harvested. Fecal DNA isolation, sequencing of 16S rRNA genes, and analysis were performed as described.[6]

Statistics

Figures and statistics were performed using GraphPad Prism 9.4.1 software. Significance level was set as $P < .05$ and all statistical tests were two-sided. All the data represent the mean ± SEM. Outliers were identified using the ROUT test (Q = 5%) and removed from the analysis. Data that were not normally distributed according to the D'Agostino & Pearson normality test were log or square root transformed, and distribution was re-assessed.

Student's *t* test or one-way/two-way ANOVA with the Tukey or Dunnett tests were used to determine significant differences between two or multiple groups, respectively. Contingency and correlation were analyzed by the Chi-square or the Fisher's exact test and the Pearson test, respectively. Survival was analyzed by the Log-rank (Mantel-Cox) test.

For the RNA-Seq, the DEGs were identified using a Benjamini-Hochberg test adjusted for false discovery rate.

The relative abundance of the genera of the intestinal microbiota was analyzed by the Wilcoxon rank sum test after multiple comparison adjustment by the Benjamini & Hochberg method.

Data Availability

RNA-Seq data can be accessed on the GEO repository using the accession number GSE201556 (token: yxybcsecfxundih). The mass spectrometry proteomics data have been deposited to the ProteomeXchange Consortium via the PRIDE partner repository with the dataset identifier PXD033228 (Reviewer account details: Username: reviewer_pxd033228@ebi.ac.uk; Password: c5NVRzhi). The 16S rRNA sequencing of the fecal microbiota has been deposited on the Sequence Read Archive website with the BioProject accession number PRJNA814820 (Temporary Submission ID: SUB11173798).

Results

DHPS Level Is Reduced in the Colon During Colitis

Utilizing RNA samples from a previous study,[27,28] we found that *DHPS* expression was reduced in colon tissues of patients with moderate and severe UC compared to normal controls (Figure 1A). This result was confirmed by previously published RNA-Seq publicly available data on the GEO website; among 7 studies with UC patients, 6 exhibited a reduced expression of *DHPS* in the colon, including 3 with significant differences (Figure 1B). In contrast, the expression of *DOHH* was not affected in UC patients (Figure 1B). Also, *DHPS* expression was reduced in each of 3 studies in the colon of CD patients, with 2 showing significant differences, while *DOHH* did not show this pattern (Figure 1B). Accordingly, we found that *DHPS* level in colonoids from patients with UC was lower compared to those from normal tissues (Figure 1C). Further, when we immunostained IBD tissue microarrays (TMAs) we observed strong DHPS and EIF5A^{Hyp} expression in CECs from normal individuals (Figure 1D), while the levels of DHPS-positive and EIF5A^{Hyp}-positive CECs were significantly reduced in patients with UC or CD (Figures 1D–E).

We then verified the level of hypusination in the colon of mice with CAC. There was a reduction of EIF5A^{Hyp} in the non-tumor tissues from AOM-DSS-treated C57BL/6 mice, and hypusination level was significantly augmented in these mice that were given the DHPS substrate, Spd (Supplementary Figure 1).

Mice with Specific Deletion of Dhps in IECs Develop Colonic Inflammation

Since patients with IBD exhibit reduced hypusination in their colon, we sought to assess the effect of epithelial-specific deletion of *Dhps* on intestinal homeostasis. Isolated CECs

from *Dhps*$^{\Delta epi}$ mice exhibited a significant reduction of *Dhps* mRNA (Figure 2A) and DHPS protein (Figures 2B–C) compared to *Dhps*$^{fl/fl}$ mice. EIF5A^{Hyp} levels were also reduced in *Dhps*$^{\Delta epi}$ CECs (Figure 2B). Using IF, we observed that EIF5A^{Hyp} was localized all along the crypts and that the staining was markedly reduced in the epithelium of *Dhps*$^{\Delta epi}$ mice (Figure 2D).

Strikingly, the colon and the cecum of *Dhps*$^{\Delta epi}$ mice exhibited a marked thickening (Figure 2E) that was confirmed by the significant increase of the colon weight/length ratio (Figure 2F). Histologically, we observed a marked expansion of the mucosal compartment (Figure 2G), confirmed by increased crypt length (Figure 2H) and by increased proliferation assessed by immunodetection (Figure 2I) and quantification (Figure 2J) of cells expressing Ki-67. The mucosal architecture of the colon of *Dhps*$^{\Delta epi}$ mice was abnormal, showing variation in crypt size and shape (Figure 2G). Crypts showed basal dilatation and bifurcation, and the luminal surface was undulating and villiform (Figure 2G); thus, crypt distortion was found in 84.6% of *Dhps*$^{\Delta epi}$ mice, whereas only 4% of *Dhps*$^{fl/fl}$ exhibited this phenotype (Figure 2K). Patchy accumulation of neutrophils and chronic inflammatory cell infiltrates were present in the lamina propria of *Dhps*$^{\Delta epi}$ mice (Figure 2G), indicating mild colitis. Accordingly, the histologic injury score was significantly higher in *Dhps*$^{\Delta epi}$ mice (Figure 2L). This was further evidenced by the significant increase of *i*) myeloperoxidase (MPO)-positive cells in the mucosa of *Dhps*$^{\Delta epi}$ mice (Supplementary Figures 2A–B) and *ii*) the expression of the genes encoding for the chemokine CXCL2, the innate effectors NOS2, TNF-α and IL-1β, and the Th1 and Th17 prototype cytokines, IFN-γ and IL-17, respectively, in the colon of *Dhps*$^{\Delta epi}$ mice (Supplementary Figure 2C). The expression of the tight junction protein ZO1 was similar in the colon of *Dhps*$^{fl/fl}$ and *Dhps*$^{\Delta epi}$ mice (Supplementary Figure 2D), suggesting that the inflammation observed in *Dhps*$^{\Delta epi}$ mice is not associated with a loss of barrier function.

In addition, we found that epithelial distortion and inflammation was also observed along the small intestine of *Dhps*$^{\Delta epi}$ mice, progressively from the duodenum and jejunum to the ileum (Supplementary Figure 3).

Deletion of Dhps in IECs Worsens DSS Colitis

Dhps$^{fl/fl}$ and *Dhps*$^{\Delta epi}$ mice were then treated with DSS to induce epithelial injury and colitis. Mortality of *Dhps*$^{\Delta epi}$ mice treated with 2% DSS was significantly increased beginning day 6 post-treatment, whereas *Dhps*$^{fl/fl}$ mice were not affected (Figure 3A). *Dhps*$^{\Delta epi}$ mice began losing weight on day 4 after starting 2% DSS, whereas *Dhps*$^{fl/fl}$ mice did not lose weight (Figure 3B). When 4% DSS was used, *Dhps*$^{\Delta epi}$ mice exhibited a rapid worsening of their condition, characterized by high mortality level (Figure 3A) and a marked body weight loss (Figure 3B). In this context, mice treated with 2% and 4% DSS were sacrificed at day 9 and day 6, respectively. The weight/length ratio of the colon (Figure 3C) and colonic inflammation and epithelial damage (Figures 3D–E) were significantly increased in *Dhps*$^{\Delta epi}$ mice vs. *Dhps*$^{fl/fl}$ animals. We also found significant increases in the expression of the proinflammatory genes *Tnf*, *Il1b*, and *Il17* in *Dhps*$^{\Delta epi}$ mice that were given 2% DSS (Figure 3F).

Increased Tumorigenesis in Dhps$^{\Delta epi}$ Mice

Since *Dhps*$^{\Delta epi}$ mice exhibit spontaneous colitis and are highly susceptible to DSS, we hypothesized that these animals would develop more tumors in the AOM-DSS model of CAC. Since we observed a high mortality rate with 2% and 4% DSS, we used 1.7% for *Dhps*$^{\Delta epi}$ mice. In fact, we observed a 100% mortality rate in *Dhps*$^{\Delta epi}$ mice after the first cycle of 1.7% DSS, whereas 90% of *Dhps*$^{fl/fl}$ animals survived the 3 cycles of 3% DSS (Supplementary Figure 4). Therefore, it was not possible to assess tumorigenesis in the *Dhps*$^{\Delta epi}$ mice in this model since the disease was so severe. We thus reasoned that the spontaneous colonic inflammation of *Dhps*$^{\Delta epi}$ mice would be sufficient to support tumor development in animals treated only with the carcinogen AOM. When *Dhps*$^{\Delta epi}$ mice received 3 injections of AOM, we observed no effect on body weight (Supplementary Figure 5A). While only 1 out of 10 *Dhps*$^{fl/fl}$ mice treated with AOM developed a tumor in the colon, 50% of the *Dhps*$^{\Delta epi}$ mice exhibited tumors (Supplementary Figure 5B) and, therefore, tumor number (Supplementary Figure 5B) and burden (Supplementary Figure 5C) were significantly increased in *Dhps*$^{\Delta epi}$ animals. After 6 injections of AOM, we did not observe a significant effect on body weight (Figure 4A). However, there was a marked increase in the number (Figures 4B and 4C) and the size (Figures 4B and 4D) of the tumors in *Dhps*$^{\Delta epi}$ mice, yielding a significant increase in the tumor burden (Figure 4E). Histologically, the injury score of the non-tumor area of the colon was significantly higher in *Dhps*$^{\Delta epi}$ mice (Figures 4F and 4G). Importantly, high-grade dysplasia (HGD) was observed in 43% of the *Dhps*$^{\Delta epi}$ mice, while only 12% of the *Dhps*$^{fl/fl}$ mice exhibited HGD (Figures 4F and 4H). Notably, we also observed one case of invasive carcinoma in the AOM-treated *Dhps*$^{\Delta epi}$ group (Figure 4F), which was included in the HGD group in Figure 4H.

Dhps Deletion in IECs Does not Modify the Gut Microbiome

We assessed the fecal microbiome of littermate *Dhps*$^{fl/fl}$ and *Dhps*$^{\Delta epi}$ mice by sequencing the V4 region of the 16S rRNA gene. Bacterial community diversity, measured by Shannon and inverse Simpson indexes (Supplementary Figure 6A), and total richness, assessed by the Chao1 index (Supplementary Figure 6B), were similar between both genotypes. As observed in C57BL/6 mice,[6] the fecal microbiota of *Dhps*$^{fl/fl}$ mice was dominated by the Bacteroidetes phylum (Supplementary Figure 6C), including the genera *Prevotella*, *Porphyromonadaceae*, and *Bacteroides* (Supplementary Figure 6D). Proteobacteria, including *Helicobacter* and *Sutterellaceae*, and Firmicutes represented by the *Oscillibacter*, *Lachnospiraceae*, and *Akkermansia* genera were also found in the fecal microbiome (Supplementary Figures 6C and 6D). The relative abundance of these genera was not significantly different between *Dhps*$^{fl/fl}$ and *Dhps*$^{\Delta epi}$ mice (Supplementary Figure 6E).

Hypusination in CECs Regulates the Translation of Enzymes Involved in Reactive Aldehyde Detoxification

To understand the mechanism by which the deletion of *Dhps* in IECs supports colitis and carcinogenesis, we analyzed the proteome of isolated CECs from 3 different mice each from the *Dhps*$^{fl/fl}$ and *Dhps*$^{\Delta epi}$ genotypes, using the isobaric tag for relative and absolute quantification (iTRAQ)-based proteomics approach. A total of 4729 proteins were identified.

Among them, 99 and 102 were significantly upregulated and downregulated, respectively, in *Dhps*$^{\Delta epi}$ versus *Dhps*$^{fl/fl}$ mice (Supplementary Table 1). The proteins induced in *Dhps*$^{\Delta epi}$ CECs included *i*) classical markers of the immune response, such as S100A8/9, NGP, and PERM, but also *ii*) signaling molecules involved in oncogenic transformation (PTN11, MMP9, RAC2), *iii*) the integrins ITB2, ITB6, and ITAM, and *iv*) Histone H2AX, a marker of DNA double strand breaks (Supplementary Table 1). The proteins downregulated with *Dhps* deletion, and thus potentially direct targets of EIF5A^{Hyp}, included *i*) MPTX and S26A2/3 that have been shown to be downregulated in colonic tumors[29] and *ii*) the keratins K2C6A, K1C16, and K2C79, which maintain normal function of the gastrointestinal epithelium (Figure 5A, Supplementary Table 1). Remarkably, we also found two types of enzymes involved in aldehyde detoxification: the aldehyde dehydrogenases (ALDHs) AL1A7, AL1B1, and ALDH2, which oxidize aldehydes to carboxylates,[30] and 6 GSTs, which catalyze the conjugation of aldehydes to glutathione,[31] including GSTA4, GSTM3, GSTM2, GSTP1, GSTO1, and GSTM1 (Figure 5A, Supplementary Table 1). Note that the expression of 3 other ALDHs (AL3B2, AL3A2, AL9A1) and 5 other GSTs (GSTK1, GSTT2, LANCL1, GSTM5, GSTT3) was reduced in *Dhps*$^{\Delta epi}$ CECs, but did not reach statistical significance (Supplementary Table 1). Importantly, all these proteins exhibited the molecular features of EIF5A^{Hyp}-regulated proteins (Supplementary Table 2), i.e., an AAAUGU consensus sequence in their mRNA[9,10,32] and/or diprolyl/diglycyl motifs in their protein.[13,14] Lastly, thioredoxin (THIO) and the peroxiredoxins 1 and 6 (PRDX1/6), which are involved in peroxide detoxification, were also significantly less expressed in *Dhps*$^{\Delta epi}$ CECs.

We found by IHC that the level of the protein GSTO1 was reduced in *Dhps*$^{\Delta epi}$ mice compared to *Dhps*$^{fl/fl}$ mice (Figure 5B), thus validating the results obtained by proteomic analysis. Importantly, the expression of *Gsto1* mRNA in isolated CECs was not affected by *Dhps* deletion (Figure 5C), further demonstrating that DHPS regulates only GST translation in CECs. Similarly, *Gsto1* and *Gstp1* mRNA levels were similar in *Dhps*$^{fl/fl}$ and *Dhps*$^{\Delta epi}$ colon organoids (Figure 5D), whereas GSTO1 and GSTP1 proteins were less expressed in colonoids derived from *Dhps*$^{\Delta epi}$ mice and in *Dhps*$^{fl/fl}$ colonoids treated with GC7 (Figures 5E and 5F). Consequently, the total GST activity was reduced with *Dhps* deletion or inhibition (Figure 5G) and the expression of *Nqo1*, a marker of electrophilic and oxidative stress,[33] was increased in naïve or stimulated *Dhps*$^{\Delta epi}$ colonoids (Figure 5H).

The differential proteome dataset from *Dhps*$^{fl/fl}$ and *Dhps*$^{\Delta epi}$ mice was then subjected to Ingenuity Pathway Analysis (IPA). Strikingly, numerous pathways related to cancer and to the immune response were significantly induced by *Dhps* deletion (Supplementary Figure 7 and Supplementary Table 3). There was also a significant dampening of only two pathways, one of which was “Conjugation of glutathione” (Supplementary Figure 7 and Supplementary Table 3), which is related to the inhibition of GST translation.

The Transcriptome of Dhps$^{\Delta epi}$ Colon Is Reshaped Toward a Pro-neoplastic State

By RNA-Seq, we identified 25,182 sequences comprising 19,498 known mRNAs and 5,684 unknown sequences (Supplementary Table 4). There were 135 and 133 differentially expressed genes (DEGs) upregulated and downregulated (2-fold or more; $P < .05$) in

Dhps$^{\Delta epi}$ mice, respectively. We observed that several genes encoding for different proteins of the extracellular matrix, including the collagen genes *Col6a1*, *Col6a2,* and *Col4a3*, the cadherin-encoding gene *Cdh11*, and the laminin gene *Lama5* were among the most induced in *Dhps*$^{\Delta epi}$ CECs (Figure 6A and Supplementary Table 4). Genes involved in signaling such as *i*) *Epha2*, encoding the receptor tyrosine kinase ephrin type-A receptor 2 that plays a role in colon carcinogenesis[34] or *ii*) *Areg* and *Ereg*, which encode amphiregulin and epiregulin, respectively, two EGF receptor ligands involved in the maintenance and progression of the tumorigenic state,[35] were also significantly induced in mice with *Dhps* deletion (Figure 6A and Supplementary Table 4). The most downregulated gene was *Exosc6*, encoding for the exosome complex component MTR3, which mediates mRNA degradation (Figure 6A and Supplementary Table 4). Additionally, different homeobox genes (*Hoxd11/12/13*), whose expression has been shown to be reduced in colitis,[6] and the genes *Pbld1/2*, encoding for the tumor suppressor phenazine biosynthesis-like domain-containing protein, were less expressed in CECs from *Dhps*$^{\Delta epi}$ mice (Figure 6A and Supplementary Table 4). None of the genes encoding for the GSTs and ALDHs were significantly affected by *Dhps* deletion (Supplementary Table 4), demonstrating that these effectors are regulated at the post-transcriptional level.

The transcriptional function of *Dhps* deletion was performed by gene set enrichment analysis (GSEA) of DEGs (Supplementary Table 5). The top signal pathways enriched in mice lacking *Dhps* in IECs were related to growth factors and to the organization of the extracellular matrix (Figure 6B), which are associated with cancer development and progression.[36] As expected, the pathways connected to RNA processing were reduced (Figure 6B).

Increased Formation of Aldehyde Adducts in Dhps$^{\Delta epi}$ Mice Supports Colonic Inflammation

Because enzymes that detoxify reactive electrophiles are less expressed in the colon of *Dhps*$^{\Delta epi}$ mice, we reasoned that reduced hypusination in IECs would be associated with oxidative covalent adduction of these aldehydes, such as isolevuglandins (isoLGs) or malondialdehydes (MDA). Using a specific single-chain fragment variable Ab (D11) that specifically recognizes adducts of isoLGs to lysine (isoLG-lysyl),[21,37] we observed increased adducts in the nuclei of CECs from naive *Dhps*$^{\Delta epi}$ mice compared to *Dhps*$^{fl/fl}$ animals (Figures 7A–B). Furthermore, we found by LC-MS that the level of adducts of MDA-dilysyl crosslinks was also significantly increased in the colon of *Dhps*$^{\Delta epi}$ mice (Supplementary Figure 8). Moreover, we observed an increase of isoLG-lysyl adducts in *Dhps*$^{fl/fl}$ animals treated with DSS, and a further enhancement in DSS-treated *Dhps*$^{\Delta epi}$ mice (Figures 7–7B). The number of isoLG-lysyl adduct-positive nuclei in the non-tumor areas was also higher in AOM-treated *Dhps*$^{\Delta epi}$ mice, whereas strong nuclear staining was observed in tumors from both genotypes (Figures 7A–B). These data indicate that dicarbonyl electrophiles are more abundant in the colon of *Dhps*$^{\Delta epi}$ mice and are more reactive in the nuclei of CECs under inflammatory stress but are present at the same level when tumors are formed.

To verify whether reactive aldehydes play a role in the pathogenesis of the colon of *Dhps*$^{\Delta epi}$ mice, we used EtHOBA, a potent scavenger of reactive aldehydes.[21,23,24] We found that EtHOBA reduced the concentration of MDA-dilysyl crosslinks in the colon of *Dhps*$^{\Delta epi}$ mice (Supplementary Figure 8). These animals were then given 2% DSS and were also maintained with or without EtHOBA. Survival (Figure 7C), colon weight/length ratio (Figure 7D), plus inflammation and epithelial damage (Figures 7E and 7F) were significantly improved when DSS-treated *Dhps*$^{\Delta epi}$ mice were given EtHOBA.

Discussion

Our study establishes that the hypusination of EIF5A in IECs is essential to limit inflammation and carcinogenesis. Mice with specific deletion of *Dhps* in IECs exhibit spontaneous colonic inflammation and crypt distortion, a hallmark of IBD histopathology. These animals are highly susceptible to DSS and are prone to develop more tumors in response to carcinogens. Mechanistically, we found that *i*) hypusination in CECs controls the translation of enzymes involved in reactive aldehyde detoxification, *ii*) there are high levels of electrophile adducts in the nuclei of *Dhps*$^{\Delta epi}$ CECs, and *iii*) treatment of *Dhps*$^{\Delta epi}$ mice with an electrophile scavenger reduces susceptibility to colitis, strongly suggesting that one of the major functions of hypusination in IECs is to prevent aldehyde-mediated oxidative damage and dampen inflammation, epithelial injury, and malignant transformation. Since we also found that UC and CD patients exhibit low levels of colonic *DHPS* mRNA, DHPS protein, and EIF5A^{Hyp}, our data imply that reduced hypusination in CECs in IBD patients may lead to increased inflammation and risk for CAC.

Supporting the concept that the DHPS-EIF5A^{Hyp} axis prevents intestinal inflammation, mice with specific deletion of *Dhps* or *Dohh* in CD4^{+} T cells develop signs of colitis and die at 10–20 wk of age.[38] However, we have reported that the deletion of *Dhps* in myeloid cells does not cause spontaneous colitis.[26] It has also been reported that putrescine produced by the gut microbiota is utilized by CECs to form Spd and EIF5A^{Hyp}, and this is associated with dampening of DSS colitis.[39] Furthermore, it has been shown that heterozygous deletion of the genes encoding for EIF5A and adenosylmethionine decarboxylase 1, which is essential for the biosynthesis of Spd, are associated with lymphoma in humans and supports lymphomagenesis in mice.[40] However, EIF5A and DHPS expression is increased in tumors[18] and hypusination correlates with poor prognosis and metastasis in several cancer types.[41,42]. In fact, knockdown of the genes encoding for proteins involved in the hypusination pathway and/or inhibition of DHPS reduce the growth of established human cancerous gastrointestinal cell lines[19,41,43,44]. Further, tumor growth and metastasis in mice are reduced when xenografts of human carcinoma cell lines are subjected to knockdown of *DHPS*[19,45] or when animals are treated with GC7 when the tumors are already formed.[19] To explain this phenotype, it has been shown hypusination supports the translation of carcinoma-specific signaling molecules such as the MYC proto-oncogene,[19] the transforming protein RHOA,[45] the inactive tyrosine-protein kinase PEAK1,[44] or the histone-lysine-specific demethylase LSD1,[43] which have been all involved in cell proliferation and metastasis. We did not find these targets in our proteomic analysis comparing CECs of *Dhps*$^{fl/fl}$ and *Dhps*$^{\Delta epi}$ mice, evidencing that the proteins regulated by hypusination in non-transformed and cancerous cells are different and may thus

have varying effects. We therefore propose that hypusination in CECs is critical to reduce colon carcinogenesis, but that once tumors are formed, EIF5A^{Hyp} in cancerous cells may sustain their growth. Fascinatingly, a similar paradox exists for polyamines: on one hand, we found that Spd dampens colon tumorigenesis,[6] but polyamines in general are required for the growth of cancerous cells.[46]

In this report, we also assessed the molecular mechanism by which *Dhps* deletion in IECs leads to intestinal inflammation and creates a pro-oncogenic state in the colon. We determined that the translation of numerous enzymes involved in detoxification of peroxide (THIO, PRDXs) and reactive aldehydes (ALDHs, GSTs), are regulated by hypusination and are thus less expressed in the colon of *Dhps*$^{\Delta epi}$ mice. Consequently, these animals exhibit increased oxidative stress/damage and inflammation. GSTs are principally localized in CECs.[47] The null genotypes of *GSTM1* or *GSTT1* have been associated with increased risk for IBD;[48] and the frequency of the *GSTT1* null genotype is significantly increased in colorectal cancer cases, but not in lung, oral, or gastric cancer.[49] Moreover, it has been shown that the protein GSTM1 is also absent in 30% and 50% of the patients with UC and colon adenocarcinoma, respectively, that harbor a *GSTM1*$^{+}$ genotype,[50] demonstrating that this enzyme is also regulated post-transcriptionally. Although numerous redundant GTSs exist, the deletion of *Gsto1* in mice is associated with susceptibility to DSS colitis[51,52] and to AOM-DSS-induced tumorigenesis.[52] Reciprocally, the local delivery of the *Gstt1* gene to mice treated with DSS dampens colitis.[53] We reported that the aldehyde isoLG is generated in the inflamed stomach and colon, and that the electrophile scavenger EtHOBA prevents dysplasia in the murine AOM-DSS model.[21] Herein, we observed increased levels of nuclear isoLG-lysyl adducts in CECs from naïve or DSS- or AOM-treated *Dhps*$^{\Delta epi}$ mice as well as a reduction of DSS-induced inflammation in *Dhps*$^{\Delta epi}$ mice treated with the electrophile scavenger EtHOBA. We also found that the adducts of the electrophile MDA to lysine were increased in the colon of *Dhps*$^{\Delta epi}$ mice and reduced by EtHOBA. All these data and our results emphasize that the defense system against reactive aldehydes in CECs is orchestrated by hypusination and help in the prevention of inflammation/carcinogenesis.

Our data establish that hypusination in CECs is essential to lower the level of spontaneous reactive aldehydes in the colonic mucosa and protects mice from colitis and colon carcinogenesis. We previously reported that Spd dampens colitis and prevents tumorigenesis in mice[6] and in the present report we further observed that hypusination is enhanced in the colonic mucosa of mice treated with Spd. Since patients with IBD exhibit reduced levels of DHPS and EIF5A^{Hyp}, restoring hypusination by Spd supplementation and/or treatment with an electrophile scavenger can be considered as rational strategies to limit oxidative damage in the colon and the risk for neoplasia.

Supplementary Material

Refer to Web version on PubMed Central for supplementary material.

Acknowledgements

We thank Dr. Venkataraman Amarnath (VUMC) for the synthesis of EtHOBA. Sequencing was performed by the Vanderbilt Technologies for Advanced Genomics (VANTAGE) core at VUMC.

Grant Support:

This work was funded by NIH grants R01DK128200 (KTW), P01CA116087 (KTW), P01CA028842 (KTW), R01DK060581 (RGM), and R01DK124906 (RGM); Veterans Affairs Merit Review grant I01CX002171 (KTW); Senior Research Award 703003 from the Crohn's & Colitis Foundation (APG and KTW); Department of Defense Peer Reviewed Cancer Research Program Impact Award W81XWH-21-1-0617 (KTW); a gift from CURE for IBD (KTW); a gift from the James Rowen Fund (KTW); the Thomas F. Frist Sr. Endowment (KTW); and the Vanderbilt Center for Mucosal Inflammation and Cancer (KTW). LAC was supported by Veterans Affairs Merit Review grant I01BX004366. YLL was supported by T32AI138932, and KMM was supported by T32CA009592. The Mass Spectrometry Core (KLS) and the Tissue Morphology Core (MKW, MBP) of the Vanderbilt Digestive Disease Research Center are supported by P30DK058404 and the Vanderbilt Ingram Cancer Center supported by NIH grant P30CA068485. Proteomics experiments were supported in part by P30DK058404 and P01CA116087. The Cooperative Human Tissue Network is supported by NIH grant UM1CA183727 (MKW).

Abbreviations used in this paper:

ALDH	aldehyde dehydrogenase
AOM	azoxymethane
CAC	colitis-associated carcinoma
CD	Crohn's disease
CECs	colonic epithelial cells
DEGs	differentially expressed genes
DHPS	deoxyhypusine synthase
DOHH	deoxyhypusine hydroxylase
DSS	dextran sulfate sodium
EIF5A	eukaryotic translation initiation factor 5A
EIF5A^{Hyp}	hypusinated EIF5A
EtHOBA	5-ethyl-2-hydroxybenzylamine
GC7	N1-guanyl-1,7-diaminoheptane
GSEA	gene set enrichment analysis
GST	glutathione-S-transferase
H&E	hematoxylin and eosin
HGD	high-grade dysplasia
IBD	inflammatory bowel disease
IEC	intestinal epithelial cells
IF	immunofluorescence
IHC	immunohistochemistry
i.p.	intraperitoneal

IPA	Ingenuity Pathway Analysis
isoLG	isolevuglandins
LGD	low-grade dysplasia
RNA-Seq	RNA sequencing
SMOX	spermine oxidase
Spd	spermidine
TMA	tissue microarray
UC	ulcerative colitis

References

1. Dahlhamer JM, Zammitti EP, Ward BW, et al. Prevalence of Inflammatory Bowel Disease Among Adults Aged >/=18 Years - United States, 2015. MMWR Morb Mortal Wkly Rep 2016; 65:1166–1169.
2. Singh P, Ananthakrishnan A, Ahuja V. Pivot to Asia: inflammatory bowel disease burden. Intestinal research 2017; 15:138–141. [PubMed: 28239326]
3. Munkholm P. Review article: the incidence and prevalence of colorectal cancer in inflammatory bowel disease. Aliment Pharmacol Ther 2003; 18 Suppl 2:1–5.
4. Wang Y, Devereux W, Woster PM, et al. . Cloning and characterization of a human polyamine oxidase that is inducible by polyamine analogue exposure. Cancer Res 2001; 61:5370–5373. [PubMed: 11454677]
5. Gobert AP, Al-Greene NT, Singh K, et al. Distinct immunomodulatory effects of spermine oxidase in colitis induced by epithelial injury or infection. Front Immunol 2018; 9:1242. [PubMed: 29922289]
6. Gobert AP, Latour YL, Asim M, et al. Protective role of spermidine in colitis and colon carcinogenesis. Gastroenterology 2022; 162:813–827 e818. [PubMed: 34767785]
7. Park MH, Cooper HL, Folk JE. Identification of hypusine, an unusual amino acid, in a protein from human lymphocytes and of spermidine as its biosynthetic precursor. Proc Natl Acad Sci U S A 1981; 78:2869–2873. [PubMed: 6789324]
8. Park JH, Aravind L, Wolff EC, et al. Molecular cloning, expression, and structural prediction of deoxyhypusine hydroxylase: a HEAT-repeat-containing metalloenzyme. Proc Natl Acad Sci U S A 2006; 103:51–56. [PubMed: 16371467]
9. Xu A, Chen KY. Hypusine is required for a sequence-specific interaction of eukaryotic initiation factor 5A with postsystematic evolution of ligands by exponential enrichment RNA. J Biol Chem 2001; 276:2555–2561. [PubMed: 11060315]
10. Maier B, Ogihara T, Trace AP, et al. The unique hypusine modification of eIF5A promotes islet beta cell inflammation and dysfunction in mice. J Clin Invest 2010; 120:2156–2170. [PubMed: 20501948]
11. Lipowsky G, Bischoff FR, Schwarzmaier P, et al. Exportin 4: a mediator of a novel nuclear export pathway in higher eukaryotes. EMBO J 2000; 19:4362–4371. [PubMed: 10944119]
12. Park MH, Wolff EC. Hypusine, a polyamine-derived amino acid critical for eukaryotic translation. J Biol Chem 2018; 293:18710–18718. [PubMed: 30257869]
13. Gutierrez E, Shin BS, Woolstenhulme CJ, et al. eIF5A promotes translation of polyproline motifs. Mol Cell 2013; 51:35–45. [PubMed: 23727016]
14. Schuller AP, Wu CC, Dever TE, et al. eIF5A functions globally in translation elongation and termination. Mol Cell 2017; 66:194–205 e195. [PubMed: 28392174]

15. Nishimura K, Lee SB, Park JH, et al. Essential role of eIF5A-1 and deoxyhypusine synthase in mouse embryonic development. Amino Acids 2012; 42:703–710. [PubMed: 21850436]
16. Park MH, Lee YB, Joe YA. Hypusine is essential for eukaryotic cell proliferation. Biol Signals 1997; 6:115–123. [PubMed: 9285094]
17. Ganapathi M, Padgett LR, Yamada K, et al. Recessive rare variants in deoxyhypusine synthase, an enzyme involved in the synthesis of hypusine, are associated with a neurodevelopmental disorder. Am J Hum Genet 2019; 104:287–298. [PubMed: 30661771]
18. Nakanishi S, Cleveland JL. Targeting the polyamine-hypusine circuit for the prevention and treatment of cancer. Amino Acids 2016; 48:2353–2362. [PubMed: 27357307]
19. Coni S, Serrao SM, Yurtsever ZN, et al. Blockade of EIF5A hypusination limits colorectal cancer growth by inhibiting MYC elongation. Cell Death Dis 2020; 11:1045. [PubMed: 33303756]
20. Levasseur EM, Yamada K, Pineros AR, et al. Hypusine biosynthesis in beta cells links polyamine metabolism to facultative cellular proliferation to maintain glucose homeostasis. Sci Signal 2019; 12.
21. Gobert AP, Boutaud O, Asim M, et al. Dicarbonyl electrophiles mediate inflammation-induced gastrointestinal carcinogenesis. Gastroenterology 2021; 160:1256–1268. [PubMed: 33189701]
22. Burgueno JF, Fritsch J, Gonzalez EE, et al. Epithelial TLR4 signaling activates DUOX2 to induce microbiota-driven tumorigenesis. Gastroenterology 2021; 160:797–808 e796. [PubMed: 33127391]
23. Carrier EJ, Zagol-Ikapitte I, Amarnath V, et al. Levuglandin forms adducts with histone H4 in a cyclooxygenase-2-dependent manner, altering its interaction with DNA. Biochemistry 2014; 53:2436–2441. [PubMed: 24684440]
24. Zagol-Ikapitte I, Amarnath V, Bala M, et al. . Characterization of scavengers of gamma-ketoaldehydes that do not inhibit prostaglandin biosynthesis. Chem Res Toxicol 2010; 23:240–250. [PubMed: 20041722]
25. Polosukhina D, Singh K, Asim M, et al. CCL11 exacerbates colitis and inflammation-associated colon tumorigenesis. Oncogene 2021; 40:6540–6546. [PubMed: 34625710]
26. Gobert AP, Finley JL, Latour YL, et al. Hypusination orchestrates the antimicrobial response of macrophages. Cell Rep 2020; 33:108510. [PubMed: 33326776]
27. Coburn LA, Horst SN, Chaturvedi R, et al. High-throughput multi-analyte Luminex profiling implicates eotaxin-1 in ulcerative colitis. PloS One 2013; 8:e82300. [PubMed: 24367513]
28. Coburn LA, Horst SN, Allaman MM, et al. L-arginine availability and metabolism is altered in ulcerative colitis. Inflamm Bowel Dis 2016; 22:1847–1858. [PubMed: 27104830]
29. Femia AP, Luceri C, Toti S, et al. Gene expression profile and genomic alterations in colonic tumours induced by 1,2-dimethylhydrazine (DMH) in rats. BMC Cancer 2010; 10:194. [PubMed: 20459814]
30. Rodriguez-Zavala JS, Calleja LF, Moreno-Sanchez R, et al. Role of aldehyde dehydrogenases in physiopathological processes. Chem Res Toxicol 2019; 32:405–420. [PubMed: 30628442]
31. Berhane K, Widersten M, Engstrom A, et al. . Detoxication of base propenals and other alpha, beta-unsaturated aldehyde products of radical reactions and lipid peroxidation by human glutathione transferases. Proc Natl Acad Sci U S A 1994; 91:1480–1484. [PubMed: 8108434]
32. Xu A, Jao DL, Chen KY. Identification of mRNA that binds to eukaryotic initiation factor 5A by affinity co-purification and differential display. Biochem J 2004; 384:585–590. [PubMed: 15303967]
33. Ross D, Siegel D. The diverse functionality of NQO1 and its roles in redox control. Redox Biol 2021; 41:101950. [PubMed: 33774477]
34. Herath NI, Boyd AW. The role of Eph receptors and ephrin ligands in colorectal cancer. Int J Cancer 2010; 126:2003–2011. [PubMed: 20039322]
35. Guzman MJ, Shao J, Sheng H. Pro-neoplastic effects of amphiregulin in colorectal carcinogenesis. J Gastrointest Cancer 2013; 44:211–221. [PubMed: 23263765]
36. Xu S, Xu H, Wang W, et al. The role of collagen in cancer: from bench to bedside. J Transl Med 2019; 17:309. [PubMed: 31521169]

37. Davies SS, Talati M, Wang X, et al. Localization of isoketal adducts in vivo using a single-chain antibody. Free Radic Biol Med 2004; 36:1163–1174. [PubMed: 15082070]
38. Puleston DJ, Baixauli F, Sanin DE, et al. Polyamine metabolism is a central determinant of helper T cell lineage fidelity. Cell 2021; 184:4186–4202 e4120. [PubMed: 34216540]
39. Nakamura A, Kurihara S, Takahashi D, et al. Symbiotic polyamine metabolism regulates epithelial proliferation and macrophage differentiation in the colon. Nat Commun 2021; 12:2105. [PubMed: 33833232]
40. Scuoppo C, Miething C, Lindqvist L, et al. A tumour suppressor network relying on the polyamine-hypusine axis. Nature 2012; 487:244–248. [PubMed: 22722845]
41. Meng QB, Kang WM, Yu JC, et al. . Overexpression of eukaryotic translation initiation factor 5A2 (EIF5A2) correlates with cell aggressiveness and poor survival in gastric cancer. PLoS One 2015; 10:e0119229.
42. Wang C, Chen Z, Nie L, et al. Extracellular signal-regulated kinases associate with and phosphorylate DHPS to promote cell proliferation. Oncogenesis 2020; 9:85. [PubMed: 32989218]
43. Li H, Wu BK, Kanchwala M, et al. YAP/TAZ drives cell proliferation and tumour growth via a polyamine-eIF5A hypusination-LSD1 axis. Nat Cell Biol 2022; 24:373–383. [PubMed: 35177822]
44. Fujimura K, Wright T, Strnadel J, et al. A hypusine-eIF5A-PEAK1 switch regulates the pathogenesis of pancreatic cancer. Cancer Res 2014; 74:6671–6681. [PubMed: 25261239]
45. Muramatsu T, Kozaki KI, Imoto S, et al. The hypusine cascade promotes cancer progression and metastasis through the regulation of RhoA in squamous cell carcinoma. Oncogene 2016; 35:5304–5316. [PubMed: 27041563]
46. Tutton PJ, Barkla DH. Comparison of the effects of an ornithine decarboxylase inhibitor on the intestinal epithelium and on intestinal tumors. Cancer Res 1986; 46:6091–6094. [PubMed: 3096554]
47. Edalat M, Mannervik B, Axelsson LG. Selective expression of detoxifying glutathione transferases in mouse colon: effect of experimental colitis and the presence of bacteria. Histochem Cell Biol 2004; 122:151–159. [PubMed: 15309552]
48. Ye X, Jiang Y, Wang H, et al. Genetic polymorphisms of glutathione S-transferases are associated with ulcerative colitis in central China. Cell Biochem Biophys 2011; 60:323–328. [PubMed: 21301992]
49. Deakin M, Elder J, Hendrickse C, et al. Glutathione S-transferase GSTT1 genotypes and susceptibility to cancer: studies of interactions with GSTM1 in lung, oral, gastric and colorectal cancers. Carcinogenesis 1996; 17:881–884. [PubMed: 8625505]
50. Barker HJ, Alpert LC, Compton CC, et al. . Loss of glutathione S-transferase (GST) mu phenotype in colorectal adenocarcinomas from patients with a GSTM1 positive genotype. Cancer Lett 2002; 177:65–74. [PubMed: 11809532]
51. Menon D, Innes A, Oakley AJ, et al. GSTO1–1 plays a pro-inflammatory role in models of inflammation, colitis and obesity. Sci Rep 2017; 7:17832. [PubMed: 29259211]
52. Tummala P, Rooke M, Dahlstrom JE, et al. Glutathione transferase Omega 1 confers protection against azoxymethane-induced colorectal tumour formation. Carcinogenesis 2021; 42:853–863. [PubMed: 33564842]
53. Kim JH, Ahn JB, Kim DH, et al. Glutathione S-transferase theta 1 protects against colitis through goblet cell differentiation via interleukin-22. Faseb J 2020; 34:3289–3304. [PubMed: 31916636]

WHAT YOU NEED TO KNOW

BACKGROUND AND CONTEXT

Hypusination is a process that controls translation of specific proteins. We determined the effect of hypusination in intestinal epithelial cells in colon homeostasis, inflammation, and cancer.

NEW FINDINGS

Patients with inflammatory bowel disease exhibit reduced hypusination, which is required to support translation of proteins involved in detoxification of reactive aldehydes, thus preventing electrophilic damage, colonic inflammation, and carcinogenesis.

LIMITATIONS

Our animal experiments focus mainly on inflammation-mediated carcinogenesis of the colon, and the role of hypusination in sporadic colorectal cancer is not addressed.

BASIC RESEARCH/CLINICAL RELEVANCE

These findings provide insights into inflammatory bowel disease pathogenesis and implicate a new mechanism by which patients with colitis have increased risk of colon cancer. Our results also suggest that restoration of hypusination or treatment with an electrophile scavenger in patients with diminished hypusination in colonic epithelial cells could represent a clinical strategy to limit colitis and prevent carcinogenesis.

LAY SUMMARY

Hypusine is a specific amino acid that is essential to limit oxidative damage in intestinal epithelial cells, thus preventing inflammation and cancer development.

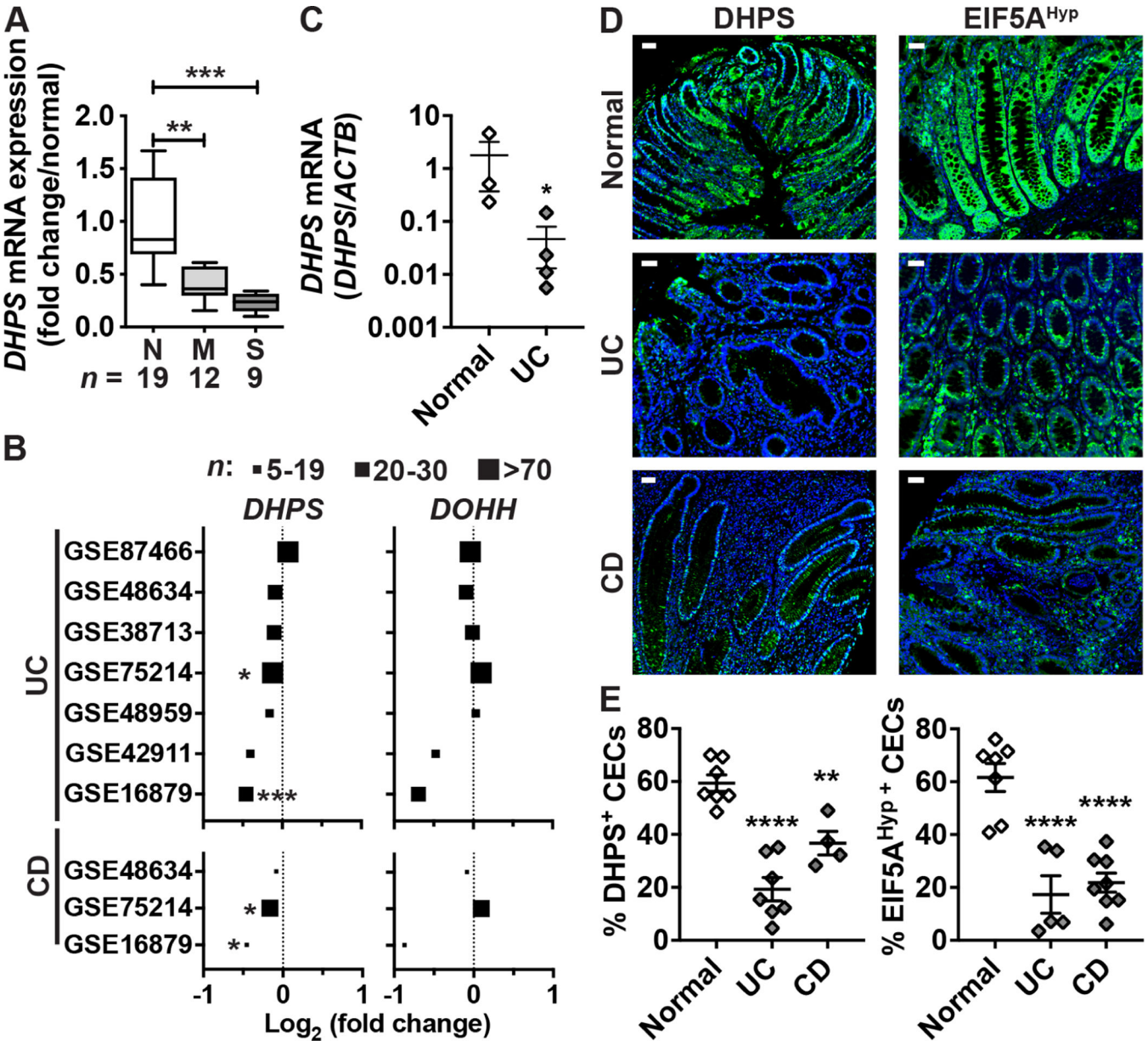

Figure 1.

Expression of *DHPS* in patients with colitis. (**A**) Total RNA was extracted from colon biopsies from normal (N; $n = 19$) or UC patients with moderate (M; $n = 12$) or severe (S; $n = 9$) colitis. *DHPS* mRNA levels were determined by RT-real-time PCR. $^{**}P < .01$, $^{***}P < .001$ by ANOVA and Tukey test. (**B**) RNA-Seq data was interrogated from published studies using the GEO data repository to determine the expression of the genes *DHPS* and *DOHH* in patients with UC or CD compared to normal individuals. *n* indicates the number of patients with colitis in each study. $^{*}P < .05$, $^{***}P < .001$ by the Benjamini & Hochberg test adjusted for false discovery rate. (**C**) *DHPS* mRNA expression was assessed by quantitative RT-PCR in colon organoids from normal or UC tissues. Each dot represents the mean of 2–3 experiments performed with colonoids from each patient; $^{*}P < .05$ using the unpaired *t* test. (**D-E**) Tissues sections of two TMAs were immunostained for DHPS or EIF5A^{Hyp}

and representative images of normal tissues ($n = 7$) or tissues from patients with UC ($n = 7$) or CD ($n = 4$) are shown in (**D**) with scale bar, 50 μm; (**E**) Quantification using QuPath of $DHPS^{+}$ and $EIF5A^{Hyp+}$ epithelial cells among total CECs on the TMAs. $^{**}P < .01$, $^{****}P < .0001$ by ANOVA and Dunnett's test.

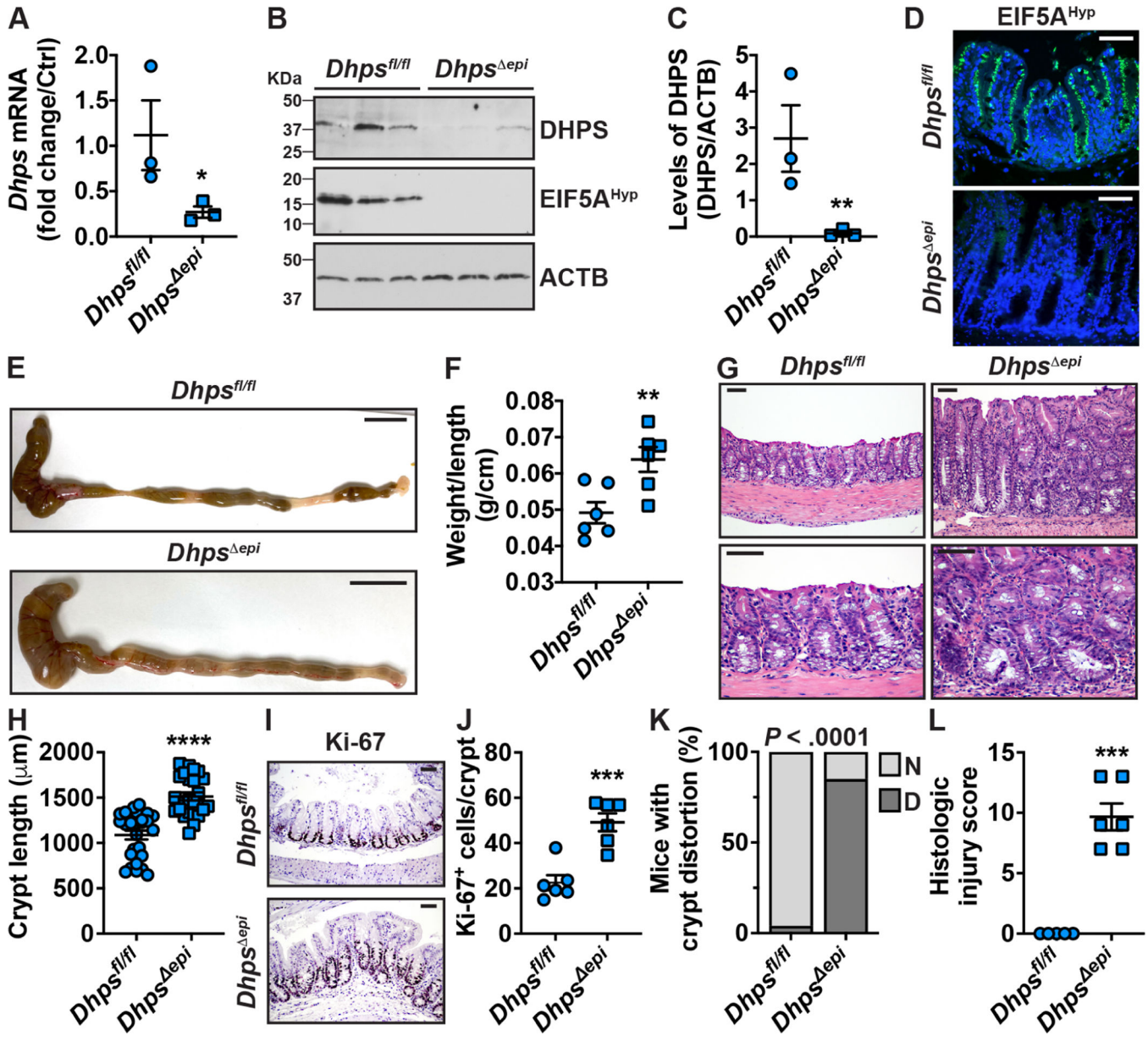

Figure 2.

Effect on the colon of the selective depletion of *Dhps* in IECs. CECs from 7-wk-old *Dhps*$^{fl/fl}$ and *Dhps*$^{\Delta epi}$ mice were isolated and the expression of *Dhps* mRNA was assessed by RT-real time PCR (**A**). The level of DHPS and EIF5A^{Hyp} was analyzed by Western blot (**B**) followed by densitometry (**C**). (**D**) IF for EIF5A^{Hyp} in the colon; representative image of 3 mice/genotype. The colon of these animals (3 males and 3 females per genotype) was removed (**E**) and length and weight were measured (**F**). Longitudinal sections were stained by H&E (**G**). Crypt length was determined using ImageJ 1.53a (n = 25–27 crypts counted from 6 different mice per genotype) (**H**). Proliferation was determined by IHC for Ki-67 (**I**) and quantification of Ki-67-positive nuclei (**J**); a total of 100 crypts were counted per mouse. The number of animals (n = 26/genotype) exhibiting normal crypt (N) or crypt distortion (D) (**K**) and the histologic injury scores (**L**) were evaluated by our pathologist in a

blinded manner. In all the panels with dot plots, *$P < .05$, **$P < .01$, ***$P < .001$, ****$P < .0001$ by unpaired Student's *t* test; in **K**, *P* was calculated using the Fisher's exact test. Scale bars represent 1 cm (**E**) or 50 μm (**D**, **G**, **H**).

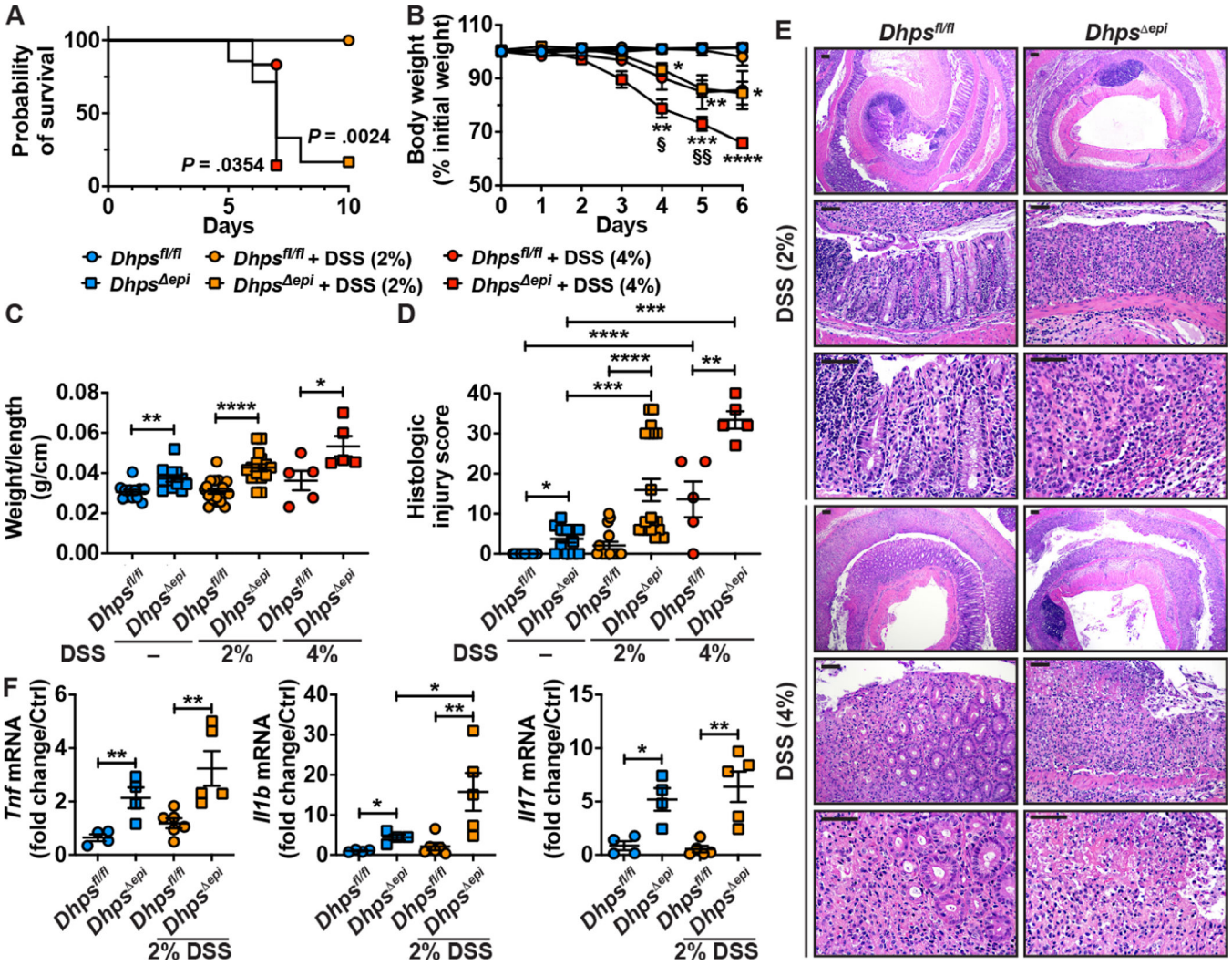

Figure 3.

DSS-induced colitis in *Dhps*$^{fl/fl}$ and *Dhps*$^{\Delta epi}$ mice. Animals were treated or not with 2% or 4% DSS. (**A**) Kaplan-Meier curves of DSS-treated mice; the *P* value was obtained using the Log-rank test (n = 7–20 mice/group). (**B**) Body weights were measured daily and are depicted as percentage of initial body weight; **P* < .05, ***P* < .01, ****P* < .001, *****P* < .0001 compared to untreated *Dhps*$^{\Delta epi}$ mice, and §*P* < .05, §§*P* < .01 versus *Dhps*$^{fl/fl}$ + 4% DSS, by two-way ANOVA and Tukey test. (**C**) Colons were harvested, washed, weighed, and measured. (**D**) Histological injury was determined from H&E staining (**E**); the scale bars on the low-power and high-power photomicrographs correspond to 100 μm and 50 μm, respectively. (**F**) mRNA expression from the colonic mucosa; *Dhps*$^{fl/fl}$ mice were used as control for the semi-quantitative analysis. In all panels with dot plots, **P* < .05, ***P* < .01, ****P* < .001 by two-way ANOVA and Tukey test.

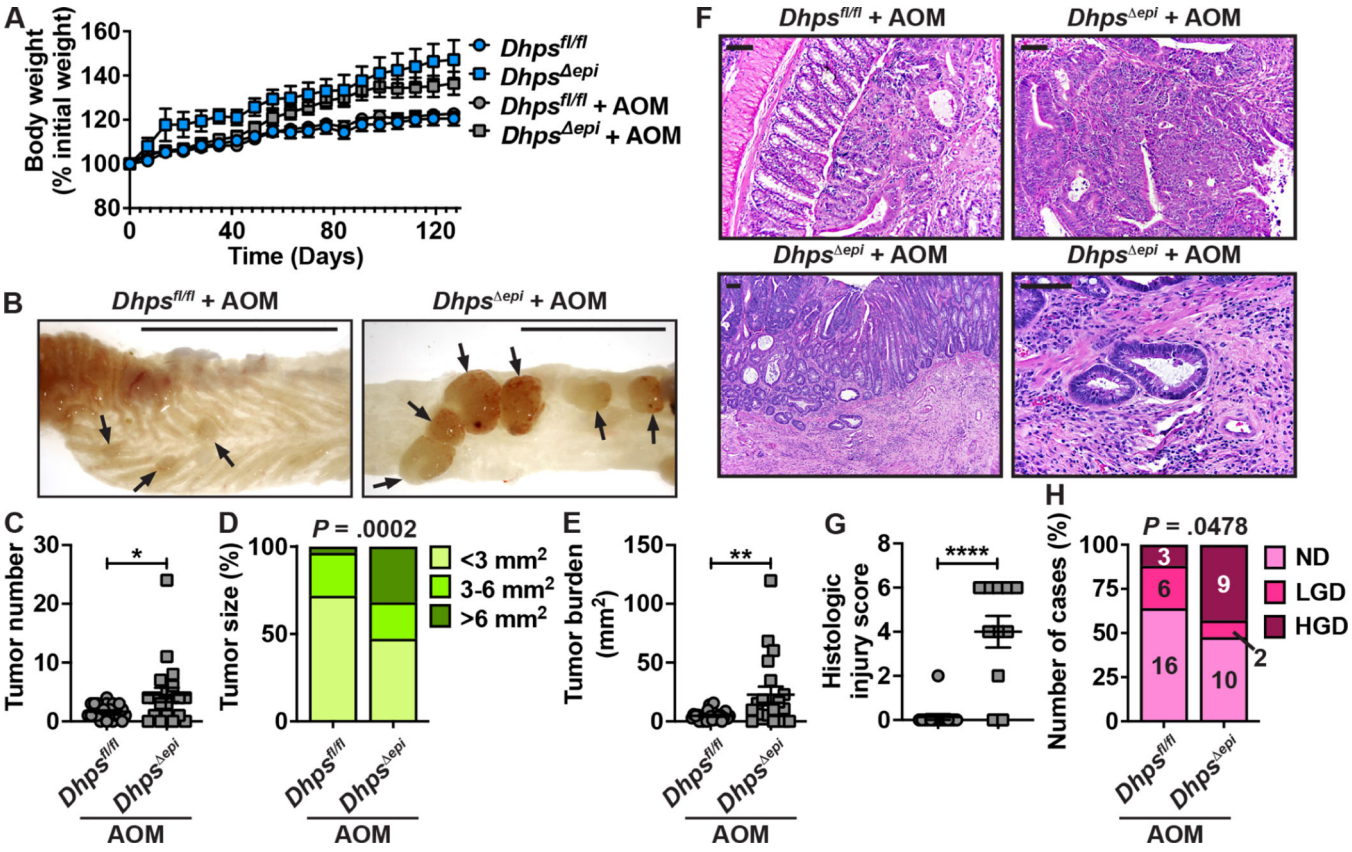

Figure 4.

Effect of epithelial *Dhps* deletion on colon carcinogenesis. $Dhps^{fl/fl}$ ($n = 25$) and $Dhps^{\Delta epi}$ mice ($n = 22$) were given 6 i.p. injections of 12.5 mg/kg AOM. Note that two $Dhps^{\Delta epi}$ mice died between day 119 and 127 ($P = 0.132$), and that none of the control animals that did not receive AOM developed tumors. (**A**) Body weights are depicted as percentage of initial body weight. (**B-E**) Colons were harvested, opened longitudinally (**B**) and tumors (arrow) were counted (**C**) and measured (**D**); in **D**, the percentages were determined from a total of 57 and 91 tumors in $Dhps^{fl/fl}$ and $Dhps^{\Delta epi}$ mice, respectively. Tumor burden (**E**) corresponds to the sum of the surface area of all the tumors in each mouse. (**F-H**) H&E staining (**F**) was used to assess histologic injury (**G**) and the grade of dysplasia (**H**). In **F**, the photomicrographs in the upper panels for $Dhps^{fl/fl}$ and $Dhps^{\Delta epi}$ mice show LGD and HGD, respectively; the lower panels depict an invasive carcinoma; scale bars, 50 μm. $^{*}P < .05$, $^{**}P < .01$, $^{****}P < .0001$ by Student's *t* test; in **D** and **H**, the *P* values were calculated using the Chi-square test.

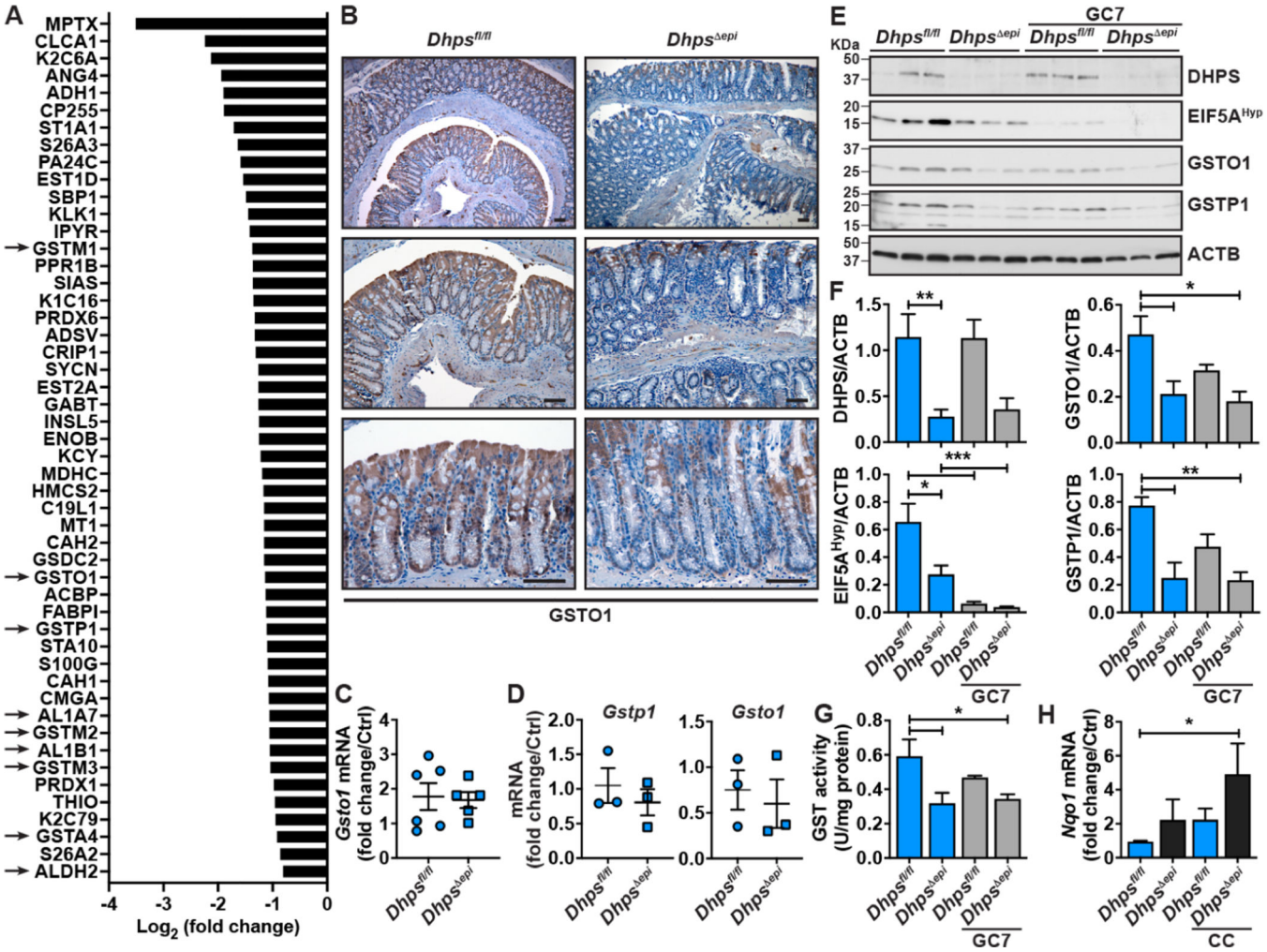

Figure 5.

Effect of hypusination on the proteome of CECs. (**A**) iTRAQ was used to determine the differential expression of the proteins from isolated *Dhps*$^{fl/fl}$ and *Dhps*$^{\Delta epi}$ CECs ($n = 3$ mice per group). This figure depicts a list of 50 proteins significantly downregulated in *Dhps*$^{\Delta epi}$ CECs compared to *Dhps*$^{fl/fl}$ control CECs; the arrows highlight the proteins involved in aldehyde detoxification. (**B**) IHC for GSTO1 in the colon of *Dhps*$^{fl/fl}$ and *Dhps*$^{\Delta epi}$ mice. These photomicrographs are representative of 6 animals per genotype; scale bars, 50 μm. The images are representatives of 5 mice/condition. (**C-D**) *Gsto1* and *Gstp1* mRNA levels in the colon (**C**) and in colonoids (**D**) of *Dhps*$^{fl/fl}$ and *Dhps*$^{\Delta epi}$ mice. (**E-F**) The level of DHPS, EIF5A^{Hyp}, GSTO1, and GSTP1 was assessed by Western blot in colonoids from *Dhps*$^{fl/fl}$ and *Dhps*$^{\Delta epi}$ mice, cultured or not for 24 h with 25 μM GC7 (**E**), followed by densitometry (**F**). (**G**) Total GST activity was determined in the same colonoids ± GC7. (**H**) Expression of the gene *Nqo1* in *Dhps*$^{fl/fl}$ and *Dhps*$^{\Delta epi}$ colonoids stimulated for 24 h with a cytokine cocktail (CC) composed of IFN-γ, IL-1β, and TNF-α. In bar graphs, $^{*}P < .05$, $^{**}P < .01$, $^{***}P < .001$ by one-way ANOVA and Dunnett's test.

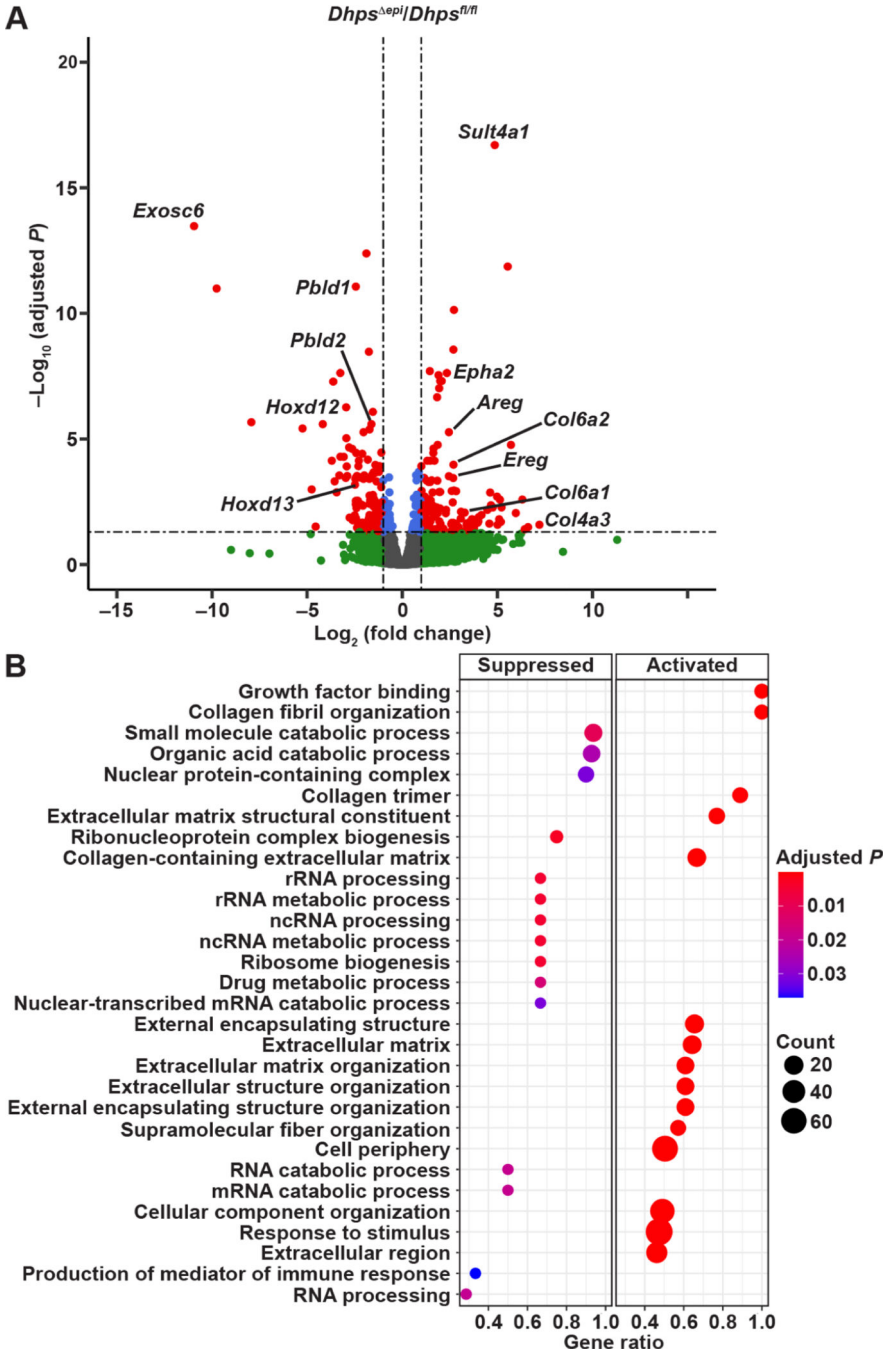

Figure 6.

Transcriptomic changes orchestrated by DHPS in CECs. (**A**) RNA extracted from CECs from *Dhps*$^{fl/fl}$ and *Dhps*$^{\Delta epi}$ (n = 3 mice per group) was sequenced, and the volcano plot corresponding to the DEGs in *Dhps*$^{\Delta epi}$ mice compared to *Dhps*$^{fl/fl}$ animals was generated using *R*; red dots correspond to genes significantly (P < .05) up- or downregulated by 2–fold or more. All the genes are provided in Supplementary Table 4. (**B**) Pathway analysis of DEGs by GSEA; the complete list of pathways is shown in Supplementary Table 5.

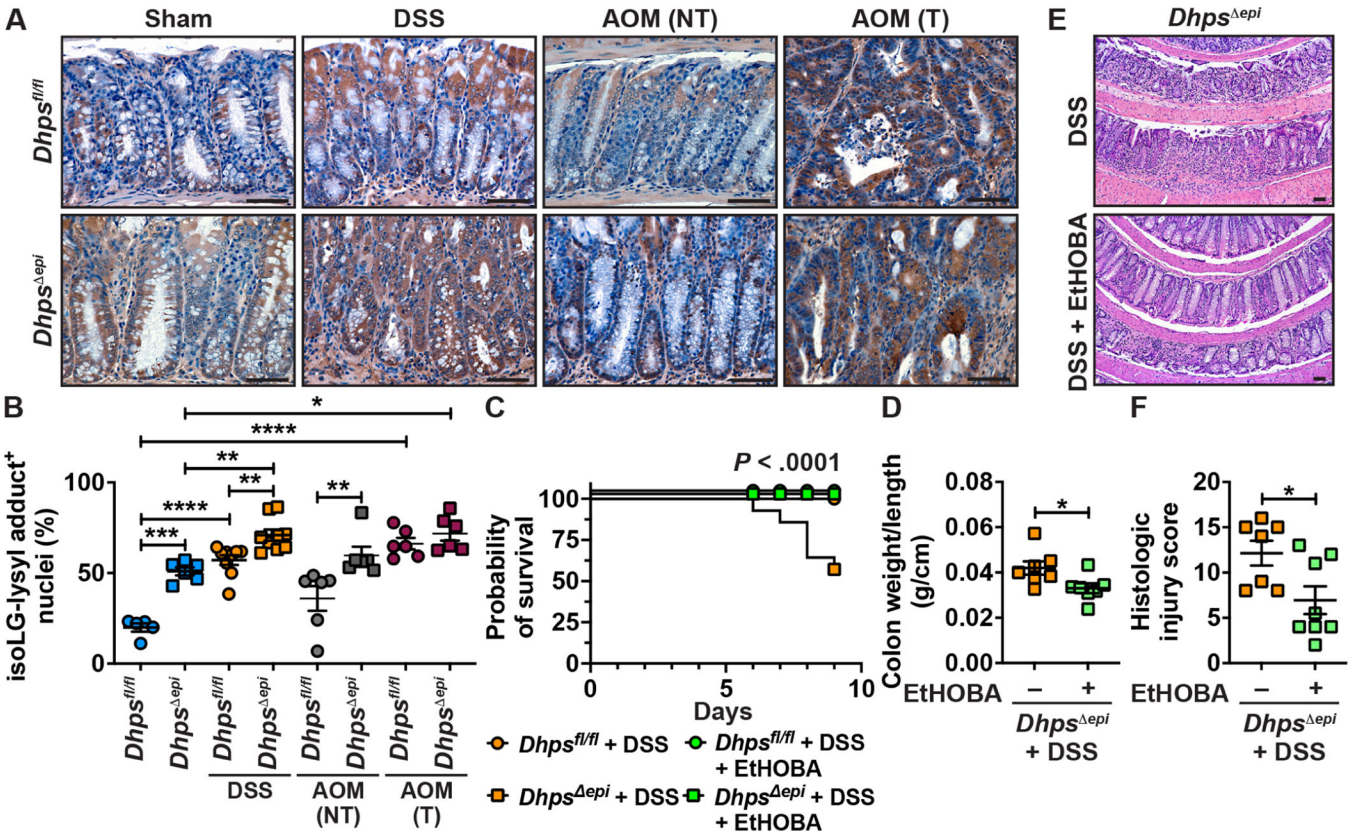

Figure 7.

Levels and role of reactive aldehydes associated with *Dhps* deletion. (**A**-**B**) The levels of isoLG-lysyl adducts in the colon of $Dhps^{fl/fl}$ and $Dhps^{\Delta epi}$ mice (n = 2–3 per group), treated or not with DSS or AOM, was assessed by immunostaining with D11 Ab and the images presented are representative of 2–3 mice/group. (**A**); the quantification of cells with positive staining for isoLG-lysyl adducts in the nucleus is shown in **B**. Each dot represents a crypt; *P < .05, **P < .01, ***P < .001, and ****P < .0001 by one-way ANOVA and Tukey test. (**C**-**F**) $Dhps^{\Delta epi}$ mice were given 2% DSS (n = 15) or DSS ± EtHOBA (n = 19). Survival was assessed by Kaplan-Meier curves and the P value was calculated by the Log-rank test (**C**); only the female mice died in this experiment. The weight and length of the colons of $Dhps^{\Delta epi}$ mice + DSS ± EtHOBA were measured and expressed as a ratio (**D**). H&E staining (**E**) was used to score histologic injury in male mice (**F**). *P < .05 by Student's t test. $Dhps^{fl/fl}$ treated with 2% DSS did not develop significant increase in histologic injury score compared to control animals, and EtHOBA had no significant effect on these mice. In **A** and **E**, the scale bars represent 50 μm.